

# Multiple mechanisms of manganese-induced quenching of fura-2 fluorescence in rat mast cells

Cristina Fasolato\*, Markus Hoth, Reinhold Penner

Department of Membrane Biophysics, Max-Planck-Institute for Biophysical Chemistry, Am Fassberg, W-3400 Göttingen, Germany

Received December 8, 1992/Received after revision January 15, 1993/Accepted January 18, 1993

**Abstract.** Whole-cell patch-clamp recordings of membrane currents and fura-2 measurements of free intracellular calcium concentration ( $[Ca^{2+}]_i$ ) were used to study  $Mn^{2+}$  influx in rat peritoneal mast cells. The calcium-selective current, activated by depletion of intracellular calcium stores ( $I_{CRAC}$  for calcium release-activated calcium current), supports a small but measurable  $Mn^{2+}$  current. In the presence of intracellular BAPTA, a  $Mn^{2+}$  current through  $I_{CRAC}$  was recorded in isotonic  $MnCl_2$  (100 mM) without a significant quenching of fura-2 fluorescence. Its amplitude was 10% of that measured in physiological solution containing 10 mM  $Ca^{2+}$ . However, following store depletion, a significant quenching of fura-2 fluorescence could be measured only when intracellular BAPTA was omitted, so that all the incoming  $Mn^{2+}$  could be captured by the fluorescent dye. Two other ionic currents activated by receptor stimulation also induced  $Mn^{2+}$  quenching of fura-2 fluorescence: a small current through non-specific cation channels of 50-pS unitary conductance and a distinct cationic current of large amplitude. In addition to these influx mechanisms,  $Mn^{2+}$  was taken up into calcium stores and was subsequently co-released with  $Ca^{2+}$  by  $Ca^{2+}$ -mobilizing agonists.

**Key words:** Calcium stores – Cation channels – Manganese quenching – Fura-2 – Patch clamp – Calcium release – Activated calcium current

## Introduction

Receptor-mediated changes in intracellular calcium concentration ( $[Ca^{2+}]_i$ ) play a pivotal role in translating extracellular signals into cellular responses. In non-excitable cells  $[Ca^{2+}]_i$  rises often show biphasic behaviour:

an initial  $Ca^{2+}$  spike that is followed by a sustained plateau phase. The former is mainly caused by release of  $Ca^{2+}$  from intracellular stores, the latter is mainly due to  $Ca^{2+}$  entry. Calcium movements across the plasma membrane can occur through several pathways including voltage-, receptor-, and second-messenger-operated channels [21, 33]. An additional mechanism of  $Ca^{2+}$  influx, mainly recognized in electrically non-excitable cells, appears to be regulated by the filling state of intracellular calcium stores [2, 28, 31].

In many cell types,  $Mn^{2+}$  seems to enter the cytosol through the same pathways as  $Ca^{2+}$  and, therefore, is often used as a surrogate of  $Ca^{2+}$  to trace receptor-stimulated  $Ca^{2+}$  influx mechanisms. The appearance of  $Mn^{2+}$  in the cytosol is reported by a quenching of fluorescence of the  $Ca^{2+}$ -indicator-dye fura-2 [7, 8]. Like  $Ca^{2+}$  influx,  $Mn^{2+}$  entry is often correlated with the filling state of intracellular  $Ca^{2+}$  stores [3, 12]. However,  $Mn^{2+}$  dye-quenching experiments cannot unambiguously discern the pathways by which  $Mn^{2+}$  (and thus  $Ca^{2+}$ ) enters the cytosol. In platelets, neutrophils, and endothelial cells,  $Mn^{2+}$  entry appears strictly to correlate with the emptiness of the  $Ca^{2+}$  stores [21]. In liver cells, receptor-activated cation channels have been suggested to account for  $Mn^{2+}$ -induced quenching of fura-2 fluorescence [13]. Recently a  $Mn^{2+}$ -permeable cation channel activated by  $[Ca^{2+}]_i$  and modulated by inositol 1,3,4,5-tetrakisphosphate ( $InsP_4$ ) has been described in endothelial cells [17]. Its activation seems to require  $[Ca^{2+}]_i$  to be raised above resting levels which, however, is not normally a prerequisite for  $Mn^{2+}$  influx [18, 24]. This suggests that there may be more than one mechanism involved in  $Mn^{2+}$  entry.

We report here that in mast cells the calcium-specific current activated by depletion of intracellular calcium stores,  $I_{CRAC}$  (calcium release-activated calcium current) [9, 10] supports a small but measurable  $Mn^{2+}$  current. We suggest that this mechanism underlies earlier observations that depletion of calcium stores induces  $Mn^{2+}$  entry [1, 3, 6, 12, 19, 29]. Furthermore, two other ionic currents activated by receptor stimulation were paral-

\* Present address: Dip. di Scienze Biomediche, Università di Padova, Via Trieste 75, 35121 Padova, Italy  
 Correspondence to: C. Fasolato

lled by  $\text{Mn}^{2+}$  quenching of fura-2 fluorescence: a small current through non-specific cation channels of 50-pS unitary conductance and a distinct cationic current of large amplitude. In addition to these influx mechanisms,  $\text{Mn}^{2+}$  can be taken up into calcium stores and be released subsequently by  $\text{Ca}^{2+}$ -mobilizing agonists.

## Materials and methods

Mast cells from rat peritoneum were obtained from ether-anaesthetized and decapitated male Wistar rats (200–300 g). A cell mixture was collected by peritoneal lavage with a Ringer's solution containing (in mM) NaCl 140, KCl 2.8,  $\text{CaCl}_2$  2,  $\text{MgCl}_2$  2, glucose 11, HEPES/NaOH 10, pH 7.2. Subsequently, mast cells were purified to more than 95% homogeneity by Percoll gradient centrifugation at 4°C for 20 min (34 000 g). The band containing mast cells was collected and resuspended in Ringer's solution of the above composition and briefly centrifuged to obtain a pellet of mast cells. The supernatant was removed and the cells were resuspended in modified medium M199 supplemented with fetal calf serum (10%),  $\text{NaHCO}_3$  (45 mM), glucose (2.5 mM), streptomycin (0.12 mg ml<sup>-1</sup>), and penicillin (0.64 mg ml<sup>-1</sup>). Finally, using this medium, mast cells were cocultured on glass coverslips with Swiss 3T3 fibroblasts and incubated at 37°C and 10%  $\text{CO}_2$ . Cells were used within 1–4 days in which time no obvious changes relevant to the phenomena described in this study were noticed.

For experiments, coverslips were transferred to the recording chamber and kept in Ringer's solution of the following composition (in mM) NaCl 140, KCl 2.8,  $\text{CaCl}_2$  10,  $\text{MgCl}_2$  2, glucose 11, HEPES/NaOH 10, pH 7.2. In some experiments the divalent ion concentration of the external solution was changed as described in the text or figure legends. Extracellular solution changes were made by local application from a wide-tipped micropipette, which contained standard Ringer's solution with various concentrations of  $\text{CaCl}_2$  and  $\text{MnCl}_2$  (as stated in the text and figure legends). Compound 48/80 (Sigma) was employed at 5–50 µg/ml. Isotonic  $\text{Mn}^{2+}$ -Ringer's solution contained (in mM)  $\text{MnCl}_2$  100, EGTA 2, glucose 11, HEPES 10, pH 7.2 (Trizma base).

The standard intracellular solution contained (in mM) potassium glutamate 145, NaCl 8,  $\text{MgCl}_2$  1, MgATP 0.5, HEPES/KOH 10, pH 7.2. Fura-2 pentapotassium salt (100 µM, Molecular Probes) was always included in the internal solution.  $\text{InsP}_3$  (10 µM, Amersham), BAPTA (10 mM, Sigma) or heparin (500 µg/ml, low molecular mass, Sigma) was added when desired.

Experiments were performed at room temperature (22–26°C) in the tight-seal whole-cell configuration of the patch-clamp technique using Sylgard-coated patch pipettes with resistances of 2–5 MΩ. Series resistances were in the range of 5–10 MΩ. High-resolution membrane currents were recorded using an EPC-9 patch-clamp amplifier (HEKA, Lambrecht, Germany) controlled by the E9SCREEN software on an Atari computer. All voltages were corrected for a liquid junction potential of 8 mV between external and internal solutions. High-resolution currents were low-pass filtered at 2.3 kHz and acquired at a sampling rate of 10 kHz, while a charting program on another computer synchronously recorded at low resolution (typically 2 Hz) parameters like holding potential, holding current (low-pass filtered at 500 Hz), fura-2 fluorescence, and timing of solution changes.

Voltage ramps were of 50 ms duration, covering a range of –100 mV to +100 mV. In most experiments, 30 voltage ramps were applied immediately after establishment of the whole-cell configuration at maximal stimulation rate (about 1.5 Hz). Capacitance and series resistance were cancelled before each voltage ramp using the automatic neutralization routine of the EPC-9 amplifier. Subsequent ramps were spaced at 10-s intervals. For analysis, the very first ramps before activation of  $I_{\text{CRAC}}$  were digitally filtered at 1 kHz, pooled and used for leak subtraction of the subsequent current records.

The holding potential was usually kept at 0 mV, because it is close to the zero-current voltage under our experimental conditions and because the electrical driving force for calcium influx at this potential is moderate enough to be coped with by the intracellularly supplied BAPTA. Current and current variance through non-selective cation channels were recorded at –40 mV, a potential chosen to minimize contaminating chloride currents, which reverse at about –40 mV. Variance analysis was performed on-line at a rate of 0.5–1 Hz by sampling 500 ms sections of membrane currents with a sampling rate of 5 kHz and low-pass filtered at 500 Hz (effective bandwidth: 2–500 Hz).

Measurement of fura-2 fluorescence from single mast cells in the whole-cell configuration was essentially as described [23]. Cells were loaded with fura-2 by diffusion from the patch pipette and  $[\text{Ca}^{2+}]_i$  was calculated from the fluorescence ratio at two excitation wavelengths (360/390 nm).

## Results

In mast cells, depletion of intracellular  $\text{Ca}^{2+}$  stores by three different experimental procedures (inositol 1,4,5-trisphosphate, ionomycin,  $\text{Ca}^{2+}$  chelators) activates a calcium current ( $I_{\text{CRAC}}$  = calcium release-activated calcium current) [9, 10]. In this study, we activated  $I_{\text{CRAC}}$  by perfusing mast cells in the whole-cell configuration of the patch-clamp technique with pipette solutions that contained inositol 1,4,5-trisphosphate ( $\text{InsP}_3$ , 10 µM) to deplete intracellular calcium stores. BAPTA (10 mM) was also included in the pipette solution, to reduce  $\text{Ca}^{2+}$ -induced inactivation of  $I_{\text{CRAC}}$  and to prevent reuptake of  $\text{Ca}^{2+}$  into the stores. The cells were bathed in isotonic  $\text{MnCl}_2$  (100 mM) to maximize inward  $\text{Mn}^{2+}$  currents. As shown in Fig. 1A, shortly after establishment of the whole-cell configuration, a small inward current appeared, presumably due to emptying of the calcium stores by  $\text{InsP}_3$ . The kinetic behaviour of the inward current activated in the presence of isotonic  $\text{MnCl}_2$  closely resembled that of  $I_{\text{CRAC}}$  carried by  $\text{Ca}^{2+}$  [9, 10]. Application of a  $\text{Mn}^{2+}$ -free Ringer's solution containing 10 mM  $\text{Ca}^{2+}$  increased the inward current, and return to the  $\text{Mn}^{2+}$  solution reversed this effect.

The current/voltage relationship of the currents in the presence of  $\text{Mn}^{2+}$  and  $\text{Ca}^{2+}$ , as assessed by a voltage-ramp protocol covering a range of –100 mV to +100 mV (Fig. 1B, left), demonstrates that both currents show inward rectification and positive reversal potentials. When scaled by a factor of 10, the ramp current obtained with  $\text{Mn}^{2+}$  superimposes well with the current recorded with  $\text{Ca}^{2+}$ , suggesting that  $\text{Mn}^{2+}$  carries only about 10% of the current through  $I_{\text{CRAC}}$ , even with the tenfold higher concentration of  $\text{Mn}^{2+}$  employed in this measurement. The current amplitudes measured at 0 mV and normalized to cell surface area (assessed by cell membrane capacitance) were  $0.11 \pm 0.02$  pA/pF (mean  $\pm$  SEM,  $n = 8$ ) for isotonic  $\text{MnCl}_2$  and  $0.43 \pm 0.04$  pA/pF (mean  $\pm$  SEM,  $n = 6$ ) for  $\text{Ca}^{2+}$  (10 mM). The latter amplitude, obtained during application of  $\text{Ca}^{2+}$ -containing solutions after development of  $I_{\text{CRAC}}$  in the presence of  $\text{Mn}^{2+}$ , is about half as large as the current amplitude measured in 10 mM  $\text{Ca}^{2+}$  without the prior superfusion of  $\text{Mn}^{2+}$ , which yielded mean current amplitudes of  $1.10 \pm 0.13$  pA/pF ( $\pm$  SEM,  $n = 13$ ). Possible expla-

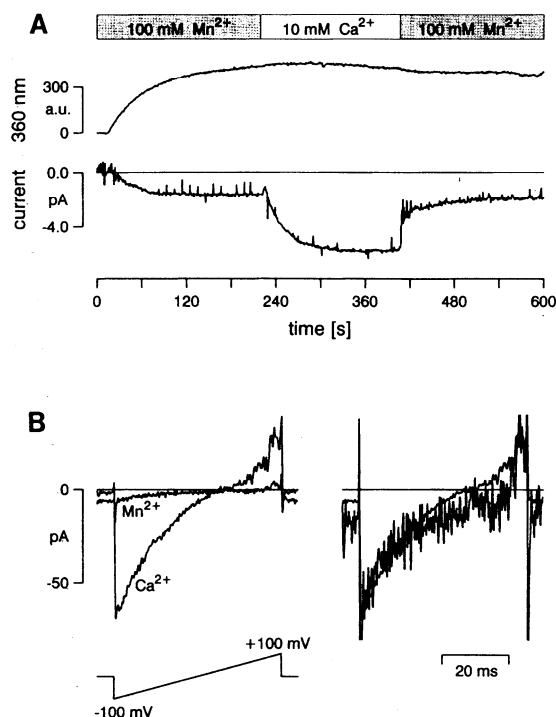


**Fig. 1 A, B.** Activation of the  $\text{Mn}^{2+}$  current by depletion of calcium stores with inositol trisphosphate ( $\text{InsP}_3$ ) and BAPTA. **A** Temporal pattern of the fura-2 signal (excited at 360 nm) and the activation of an inward current recorded at 0 mV holding potential and sampled at 2 Hz. The cell was perfused in the whole-cell configuration of the patch-clamp technique with the standard patch pipette solution supplemented with  $\text{InsP}_3$  (10  $\mu\text{M}$ , Amersham) and BAPTA (10 mM). Shortly after patch rupture (indicated by the rise in the 360-nm fura-2 signal), a small inward current, carried by  $\text{Mn}^{2+}$ , developed (the extracellular solution was isotonic 100 mM  $\text{MnCl}_2$ ). Its amplitude was increased by changing the bath solution from isotonic  $\text{MnCl}_2$  to a  $\text{Ca}^{2+}$ -Ringer's solution (containing 10 mM  $\text{CaCl}_2$ ). The spikes in the current trace reflect occasional and poorly resolved sampling of currents in response to voltage ramps as shown in **B**. **B** Single high-resolution currents during voltage ramp pulses from  $-100$  mV to  $+100$  mV (duration: 50 ms). The *left panel* depicts current traces in response to such voltage pulses recorded in the presence of isotonic  $\text{MnCl}_2$  and during 10 mM  $\text{Ca}^{2+}$ -Ringer's application. The *right panel* shows the same current traces but with the  $\text{Mn}^{2+}$  current trace scaled up by a factor of 10. All current traces were leak-corrected by subtracting ramp currents obtained before activation of the inward current (for details see [9, 10]).

nations for this may be sought in incomplete washout of  $\text{Mn}^{2+}$  or toxic effects of  $\text{Mn}^{2+}$  entering the cell.

In the experiments described above, fura-2 (100  $\mu\text{M}$ ) was included in the pipette solution. Its diffusion into the cell is seen as an exponential increase in the fluorescence at 360 nm, the isosbestic point of fura-2 (Fig. 1A). During the exchange of  $\text{Mn}^{2+}$ - and  $\text{Ca}^{2+}$ -containing ( $\text{Mn}^{2+}$ -free) solutions, there was no significant change of fura-2 fluorescence despite the flow of  $\text{Mn}^{2+}$  ions through  $I_{\text{CRAC}}$ . Presumably, the lack of substantial fluorescence quenching is mainly due to a high BAPTA concentration (10 mM) present in the internal solution, which will effectively chelate incoming  $\text{Mn}^{2+}$  and prevent its binding to fura-2.

The previous experimental conditions were optimized for measuring  $\text{Mn}^{2+}$  currents through  $I_{\text{CRAC}}$ . In order to enhance detection of  $\text{Mn}^{2+}$ -induced fluorescence quenching we omitted any  $\text{Ca}^{2+}$  chelators competing with fura-2 from the pipette solution. Figure 2A illustrates experiments carried out in Ringer's solutions containing  $\text{Ca}^{2+}$  alone (2 mM) or  $\text{Mn}^{2+}$  alone (1 mM), while  $\text{InsP}_3$  was perfused intracellularly to deplete calcium stores. The fura-2 fluorescence was monitored while the cell was subjected to periodic shifts of the membrane potential to change the electrical driving force for cation influx across the membrane. In the presence of extracellular  $\text{Ca}^{2+}$ , hyperpolarizing pulses were accompanied by transient decreases of fluorescence in the  $\text{Ca}^{2+}$ -sensitive wavelength of fura-2 (390 nm) with no change in the signal corresponding to 360 nm (the isosbestic point of fura-2), resulting in periodic increases of the calculated  $[\text{Ca}^{2+}]_i$  (Fig. 2A, left panel). Under the same conditions but with  $\text{Mn}^{2+}$  in the bath, similar fluorescence transients followed the steps to negative membrane potential, but at both wavelengths, indicative of  $\text{Mn}^{2+}$ -induced quenching of fluorescence. Since both wavelength signals were equally affected, there was no change in the calculated  $[\text{Ca}^{2+}]_i$  trace (Fig. 2A, middle panel). The overall fluorescence observed in the presence of  $\text{Mn}^{2+}$  was reduced by  $48 \pm 11\%$  (mean  $\pm$  SEM,  $n = 5$ ) compared to the fluorescence measured after return to  $\text{Ca}^{2+}$ -Ringer's solution (data not shown). This is probably due to a steady influx of  $\text{Mn}^{2+}$  through  $I_{\text{CRAC}}$  arising from the electrochemical gradient. The control experiment demonstrates that, in the absence of  $\text{InsP}_3$ , there is no detectable voltage-induced  $\text{Mn}^{2+}$  quenching of fluorescence (Fig. 2A, right panel). However, in the presence of  $\text{Mn}^{2+}$  the overall fluorescence at 360 nm was reduced by  $11 \pm 6\%$  (mean  $\pm$  SEM,  $n = 3$ ) by the basal quenching due to  $\text{Mn}^{2+}$  leakage. Therefore, the net quenching of fura-2 in the steady state is about 37%.

An experiment that shows the close correlation of  $\text{Ca}^{2+}$  and  $\text{Mn}^{2+}$  influx is illustrated in Fig. 2B. The cell was perfused with  $\text{InsP}_3$  (10  $\mu\text{M}$ ) in the presence of  $\text{Ca}^{2+}$  in the bath solution. The resulting depletion of calcium stores presumably triggered  $I_{\text{CRAC}}$ , as demonstrated by oscillating changes in  $[\text{Ca}^{2+}]_i$  that closely follow the variations in membrane potential. These transients ride on top of a slow "wave", which slowly returns to baseline and the envelope of which presumably reflects the time course of  $I_{\text{CRAC}}$  under these experimental conditions. A  $\text{Ca}^{2+}$ -free Ringer's solution containing 1 mM  $\text{Mn}^{2+}$  was applied twice, at the peak of the  $\text{Ca}^{2+}$  influx wave and after its decline. The fluorescence decrease induced by  $\text{Mn}^{2+}$  entry was larger at the peak and smaller at the end of the wave, paralleling the magnitude of  $\text{Ca}^{2+}$  influx.

Fluorescence quenching by  $\text{Mn}^{2+}$  is frequently observed following agonist stimulation and may involve multiple mechanisms. When stimulating mast cells with the secretagogue 48/80 (5  $\mu\text{g}/\text{ml}$ ), we observed two additional mechanisms for  $\text{Mn}^{2+}$  entry and fluorescence quenching of fura-2 (Fig. 3). In this type of experiment, we included heparin (500  $\mu\text{g}/\text{ml}$ ) in the pipette, which antagonized the  $\text{InsP}_3$ -induced calcium release normally

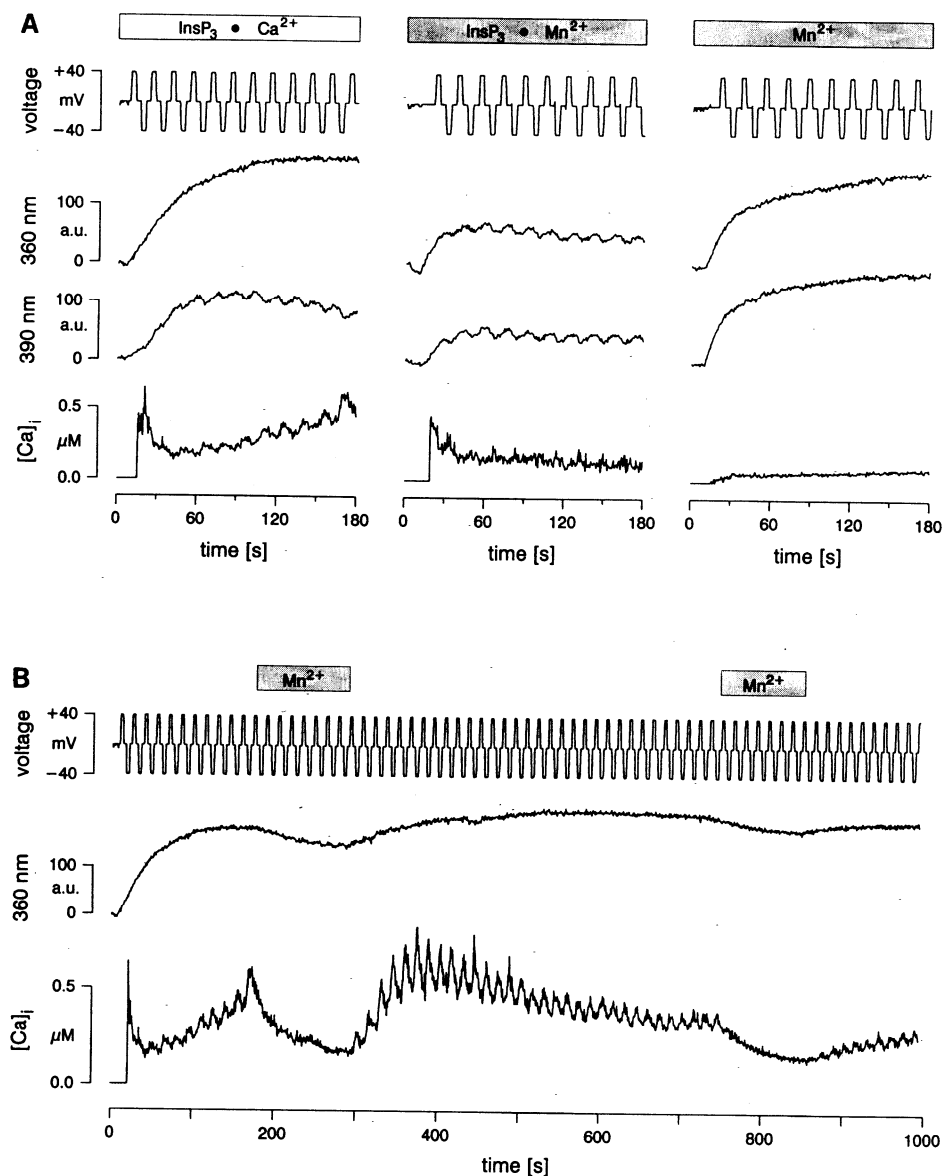


**Fig. 2 A, B.** Fluorescence quenching of fura-2 by  $Mn^{2+}$  influx induced by depletion of calcium stores with  $InsP_3$ . **A** Changes in the fura-2 signal (360 nm and 390 nm) and the resulting  $[Ca^{2+}]_i$  under conditions where the electrical driving force for divalent ion fluxes was varied by regular changes in membrane voltage.  $InsP_3$  (10  $\mu M$ ) was included in the standard intracellular solution (*left and middle panels*), resulting in a fast calcium transient followed by a sustained phase of  $Ca^{2+}$  influx (*left panel*; 2 mM  $Ca^{2+}$  in standard Ringer's solution) or  $Mn^{2+}$  influx (*middle panel*: 1 mM  $Mn^{2+}$  and 0.1 mM EGTA in  $Ca^{2+}$ -free Ringer's solution). The *right panel* shows the absence of  $Mn^{2+}$  quenching when  $InsP_3$  is omitted from the patch-pipette. **B** Correlation of the magnitude of  $Ca^{2+}$  and  $Mn^{2+}$  influx using experimental conditions as in **A**.  $Mn^{2+}$  quenching was monitored by changes in the fluorescence signal at 360 nm and  $Ca^{2+}$  influx by changes in the calculated ratio (360/390 nm). The cell was bathed in  $Ca^{2+}$ -Ringer's solution (2 mM  $Ca^{2+}$ ) and perfused with the standard intracellular solution containing  $InsP_3$  (10  $\mu M$ ).  $Mn^{2+}$  influx was induced twice (at the peak and the decay phase of  $Ca^{2+}$  influx) by applying a  $Ca^{2+}$ -free Ringer's solution containing 1 mM  $Mn^{2+}$  and 0.1 mM EGTA.

seen with the agonist [4], and thereby precluded the activation of  $I_{CRAC}$ . There was, however, a small inward current (magnified inset in Fig. 3) during the first brief application of a solution containing 48/80 and  $Mn^{2+}$ . This current was carried by previously characterized non-selective cation channels of 50-pS unitary conductance [20, 25] and produced a small increase in the current variance. Although most of the current was probably carried by monovalent cations, presumably there was also a small flux of  $Mn^{2+}$  through these channels, since the fluorescence signal at 360 nm underwent a transient decrease.

The second longer application of the same solution this time activated an additional large inward current (see Fig. 3). This was accompanied by a fast and complete quenching of fluorescence, which recovered when the application of  $Mn^{2+}$  ceased. Subsequently there was an increase in  $[Ca^{2+}]_i$ , caused by renewed influx of  $Ca^{2+}$ , which was present in the normal bath solution. This cur-

rent was not observed as regularly as the 50-pS cation channels (50% and 81%, respectively; 32 cells); when it was activated, it was accompanied by a larger current variance as compared to the current carried by 50-pS channels and showed a great deal of variability in both kinetics and amplitude. The current did not seem to be activated by a rise in  $[Ca^{2+}]_i$  (cf. the calcium trace in Fig. 3). Once activated, we rarely saw the current return to pre-stimulus values, which discouraged us from investigating this current in great detail.

In addition to stimulated  $Mn^{2+}$  entry, there is also  $Mn^{2+}$  uptake of the resting cell [3]. We tested for possible uptake of  $Mn^{2+}$  into calcium stores by preincubating mast cells in isotonic  $MnCl_2$  for 4–5 min and then challenging them with an agonist in  $Mn^{2+}$ -free Ringer's solution. Figure 4 shows that the agonist 48/80 (5  $\mu g/ml$ ) induced a  $Ca^{2+}$  transient by releasing  $Ca^{2+}$  from intracellular stores in both untreated and  $Mn^{2+}$ -preincubated cells. Note, however, that the fura-2 fluorescence mea-

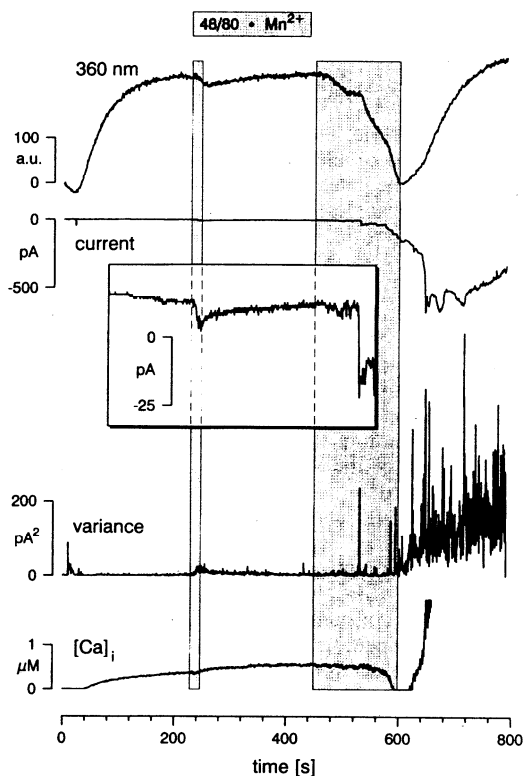


**Fig. 3.** Agonist-induced  $\text{Mn}^{2+}$  quenching of fura-2 fluorescence. Fluorescence at 360 nm, current at  $-40$  mV holding potential, current variance, and  $[\text{Ca}^{2+}]_i$  were recorded during perfusion with the standard intracellular solution supplemented with heparin 5271 ( $500 \mu\text{g}/\text{ml}$ , Sigma). The standard bathing solution (Ringer's solution with  $1 \text{ mM } \text{Ca}^{2+}$ ) was replaced during the indicated times by local perfusion of the agonist compound 48/80 ( $5 \mu\text{g}/\text{ml}$ , Sigma) in a  $\text{Ca}^{2+}$ -free Ringer's solution that also contained  $1 \text{ mM } \text{Mn}^{2+}$  and  $0.1 \text{ mM}$  EGTA. The first application of the agonist resulted in  $\text{Mn}^{2+}$ -induced quenching of the fura-2 fluorescence (upper panel) by a small inward current (see magnified inset) that was due to activation of  $50\text{-pS}$  cation channels with a characteristic change in current variance (described in detail in [20, 25]). The second, more prolonged application induced an additional large inward current with an increased current variance. Current variance was used to distinguish the two cation currents

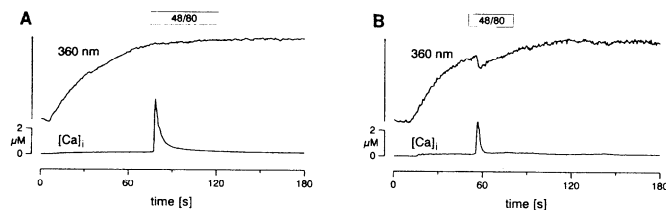


**Fig. 4 A, B.**  $\text{Mn}^{2+}$  release in response to agonist stimulation. Changes in the fura-2 signal at 360 nm and in  $[\text{Ca}^{2+}]_i$  induced by application of 48/80 ( $5 \mu\text{g}/\text{ml}$ ) in the absence of extracellular  $\text{Mn}^{2+}$ . Cells were perfused with the standard intracellular solution via the patch pipette and then stimulated with the agonist (holding potential was  $0 \text{ mV}$ ). **A** Control experiment in standard  $\text{Ca}^{2+}$ -Ringer's solution ( $2 \text{ mM } \text{Ca}^{2+}$ ) without  $\text{Mn}^{2+}$  pretreatment. **B** Conditions as before, but prior to agonist stimulation the cell had been exposed to isotonic  $\text{MnCl}_2$  ( $100 \text{ mM}$ ) for  $4 \text{ min}$  after which it was thoroughly washed and kept in a standard  $\text{Mn}^{2+}$ -free  $\text{Ca}^{2+}$ -Ringer's solution ( $2 \text{ mM } \text{Ca}^{2+}$ )

sured at the isosbestic point ( $360 \text{ nm}$ ) was decreased only in the  $\text{Mn}^{2+}$ -pretreated cells. This result suggests that  $\text{Mn}^{2+}$  can be taken up into the stores like other divalent cations [16, 22, 24], and is co-released with  $\text{Ca}^{2+}$  from the stores by  $\text{InsP}_3$ -generating agonists.

## Discussion

One important finding of this study is that the calcium release-activated calcium current in mast cells ( $I_{\text{CRAC}}$ ) can support a small but measurable  $\text{Mn}^{2+}$  current. The influx of  $\text{Mn}^{2+}$  can be detected either by direct measurement of the current or by monitoring the  $\text{Mn}^{2+}$  quenching of fura-2 fluorescence; however, conditions favouring one type of measurement preclude the other.

Since  $\text{Mn}^{2+}$  currents through  $I_{\text{CRAC}}$  are extremely small, a direct demonstration of the  $\text{Mn}^{2+}$  current was performed under conditions where the extracellular medium consisted of isotonic  $\text{MnCl}_2$  and the intracellular solution contained BAPTA to boost inward current through  $I_{\text{CRAC}}$ . In agreement with our earlier findings [9], there was only a minor quenching of fura-2 under these conditions. Several factors may contribute to this observation. First, the amount of incoming  $\text{Mn}^{2+}$  is only about 10% of the incoming  $\text{Ca}^{2+}$  even when isotonic  $\text{MnCl}_2$  was used. Second,  $\text{Mn}^{2+}$  ions will not be able to quench fura-2 significantly, because most of them will be absorbed by the 100-fold higher concentration of BAPTA. Third, there is a constant perfusion of the cell through the fura-2-containing patch pipette, which will effectively exchange quenched dye molecules and further mask the small quenching effect.

The ability of  $\text{Mn}^{2+}$  to quench fura-2 fluorescence is readily seen when BAPTA is omitted from the intracellular solution, even when a smaller  $\text{Mn}^{2+}$  concentration is used in the extracellular solution (cf. Fig. 2). In this situation, the only factor that will attenuate the quenching effect is provided by the constant perfusion of the cell with fura-2-containing solution. The fact that  $I_{\text{CRAC}}$  carries  $\text{Mn}^{2+}$  ions may account for  $\text{Mn}^{2+}$  quenching of fura-2 fluorescence induced by depletion of intracellular  $\text{Ca}^{2+}$  stores. It readily fits with the data obtained by using thapsigargin, cyclopiazonic acid, and 2,5-di-*tert*-butylhydroquinone, which are thought to deplete the stores passively by interfering with microsomal  $\text{Ca}^{2+}$  pumps [31, 32]. Moreover, we estimated a  $\text{Mn}^{2+}$  quenching rate constant ( $k = 0.012 \text{ s}^{-1}$ ) due to  $I_{\text{CRAC}}$  that is in good agreement with that found by Jacob in endothelial cells, loaded with fura-2 ester, during activation of  $\text{Mn}^{2+}$  influx by store depletion ( $k = 0.014 \text{ s}^{-1}$ , see [12]). The details of the calculations are described in the Appendix.

In mast cells we have found two additional sources of  $\text{Mn}^{2+}$  influx following agonist stimulation. One is provided by  $50\text{-pS}$  cation channels, which are activated by secretagogues [25], and the other, less well-characterized cation current, is more frequently observed after prolonged stimulation with 48/80. The  $50\text{-pS}$  cation channels are presumably activated through a GTP-binding protein and are likely to be part of the physiological response of mast cells to secretagogues [15, 20]. This is

less clear for the large cation current, because its activation was not readily reversible in our experiments. We do not know whether this current is activated in more physiological conditions in intact cells, but since we did not observe its activation in the absence of agonist stimulation, we think it is a cellular response, which may be pathological, but not simply a breakdown of the pipette/membrane seal. Furthermore, activation of more than one channel by 48/80 was also recently suggested using noise analysis [14].

Numerous studies have found  $Mn^{2+}$  quenching following receptor stimulation by  $InsP_3$ -generating agonists [21]. In addition to depleting  $Ca^{2+}$  stores, these agonists may also activate other mechanisms contributing to  $Mn^{2+}$  influx, such as receptor-activated cation channels. In some cell types,  $InsP_4$  has been reported to enhance  $Ca^{2+}$  influx [11, 26]. The action of  $InsP_4$  normally seems to require the additional presence of  $InsP_3$  [5, 27, 30]. A direct demonstration of  $Mn^{2+}$  currents through cation channels comes from endothelial cells stimulated by extracellular ATP [17]. These channels were activated by elevated  $[Ca^{2+}]_i$  and their open probability was enhanced by  $InsP_4$ ; apparently there was no additional requirement for  $InsP_3$ . Since these channels were dependent on elevated levels of  $[Ca^{2+}]_i$ , they are likely not to be responsible for  $Mn^{2+}$  quenching following depletion of  $Ca^{2+}$  stores, as this can occur at resting levels of  $[Ca^{2+}]_i$  [12, 18, 24] (this study). In mast cells we have not been able to find any effects of  $InsP_4$  on  $Ca^{2+}$  or  $Mn^{2+}$  influx. Neither 50-pS cation channels [20, 25] nor  $I_{CRAC}$  are activated or modulated by  $InsP_4$  [9] (unpublished observations). Furthermore, 50-pS channels and  $I_{CRAC}$  are not activated but inhibited by elevations of  $[Ca^{2+}]_i$  [10, 20] and  $I_{CRAC}$  is activated by store depletion, which may be induced by procedures that do not involve inositol phosphates at all (e. g. ionomycin or  $Ca^{2+}$  chelators) [9, 10].

Thus, although  $InsP_4$  may play a supporting role in  $Ca^{2+}$  and  $Mn^{2+}$  influx in some cell types it does not seem to do so in all cells, whereas  $Ca^{2+}$  and  $Mn^{2+}$  influx following store depletion is recognized as a wide-spread phenomenon [11, 28]. This would suggest that  $I_{CRAC}$  may be a rather ubiquitous mechanism by which non-excitable cells accomplish  $Ca^{2+}$  influx to refill depleted calcium stores. In fact, some of our preliminary experiments revealed calcium inward currents resembling  $I_{CRAC}$  in a variety of cell types, including RBL-2H3 (rat basophilic leukemia), 3T3 fibroblasts, dissociated thyrocytes, hepatocytes, and HL-60 (human leukemia cells). Furthermore, we found additional sources of receptor-mediated  $Mn^{2+}$  entry and release. Since these or alternative pathways may be present in other cells, one should be cautious in interpreting the effects of  $Mn^{2+}$  in terms of a single mechanism.

**Acknowledgements.** We thank E. Neher for numerous helpful comments on the manuscript and M. Pilot for his technical assistance. We gratefully acknowledge support by the following institutions: Deutsche Forschungsgemeinschaft, Sonderforschungsbereich 236, Hermann- und Lilly-Schilling-Stiftung (to R. P.), and the European Molecular Biology Organization (EMBO) (to C. F.).

## Appendix

### Calculation of the $Mn^{2+}$ quenching rate constant

Fura-2 quenching experiments in the whole-cell configuration of the patch-clamp technique should take into account the diffusion between the cytosol and the patch pipette. We assumed that (a) all incoming  $Mn^{2+}$  will be captured by the fura-2 (because of the high affinity of fura-2 for  $Mn^{2+}$ ), (b) there is no extrusion and sequestration of  $Mn^{2+}$ , (c) the diffusion rate of the fura-2- $Mn^{2+}$  complex into the pipette is equal to that of fura-2 itself, (d) fura-2 loading and unloading rates are equal, and (e) there is no backward flux of the fura-2- $Mn^{2+}$  complex from the pipette to the cytosol, considering the fact that the volume of the pipette is infinite compared to that of the cell. When  $Mn^{2+}$  quenching was measured under steady-state conditions (see Fig. 2A) the influx of  $Mn^{2+}$  from the extracellular medium to the cytosol should then have been equal to the efflux of the fura-2- $Mn^{2+}$  complex from the cytosol to the patch pipette:

$$k_{Mn}[Mn^{2+}]_{out} = k_F[F-Mn], \quad (1)$$

where  $k_{Mn}$  is the rate constant of  $Mn^{2+}$  influx into the cytosol across the cell membrane,  $[Mn^{2+}]_{out}$  is the extracellular  $Mn^{2+}$  concentration,  $k_F$  is the rate constant of fura-2 unloading (diffusion from the cytosol to the pipette), and  $[F-Mn]$  is the concentration of the fura-2- $Mn^{2+}$  complex inside the cell. We estimated the rate constant of diffusion of fura-2,  $k_F$ , from the differential equation for the unloading of the fura-2:

$$d/dt([fura-2]) = -k_F[fura-2], \quad (2)$$

where  $[fura-2]$  is the fura-2 concentration in the pipette. Both rate constants,  $k_{Mn}$  and  $k_F$ , have to be understood as normalized to the cell volume. This equation is solved by an exponential function where the time constant  $\tau$  is given by

$$\tau = 1/k_F. \quad (3)$$

The  $Mn^{2+}$  quenching rate constant  $k$  is defined as the  $Mn^{2+}$  influx divided by the amount (mol) of fura-2 inside the cell ( $[fura-2] \times \text{cell volume}$ ). However, the cell volume does not appear explicitly in the formula (Eq. 4), because  $k_{Mn}$  itself is normalized to the cell volume:

$$k = (k_{Mn}[Mn^{2+}]_{out})/[fura-2]. \quad (4)$$

Inserting Eqs. (1) and (3) in Eq. (4), we calculated  $k$  to be equal to

$$k = (1/\tau)[F-Mn]/[fura-2]. \quad (5)$$

The time constant  $\tau$  was measured from the loading of fura-2 into the cell by fitting an exponential to the time course for the fluorescence increase at 360 nm after breaking into the cell ( $\tau = 30 \pm 1$  s, mean  $\pm$  SEM,  $n = 16$ ). The concentration of fura-2 in the pipette,  $[fura-2]$ , was always 100  $\mu$ M. The concentration of the fura-2- $Mn^{2+}$  complex,  $[F-Mn]$ , at steady-state quenching was estimated to be equal to 37  $\mu$ M (37% of the fura-2 in the cell was quenched in steady state, see Results). Inserting these values in Eq. (5) yields  $k = 0.012$  s $^{-1}$ .

## References

1. Alvarez J, Montero M, Garcia-Sancho J (1992) Cytochrome P450 may regulate plasma membrane  $Ca^{2+}$  permeability according to the filling state of the intracellular  $Ca^{2+}$  stores. *FASEB J* 6: 786–792
2. Casteels R, Droogmans G (1981) Exchange characteristics of the noradrenaline-sensitive calcium store in vascular smooth muscle cells or rabbit ear artery. *J Physiol (Lond)* 317: 263–279
3. Clementi E, Scheer H, Zacchetti D, Fasolato C, Pozzan T, Meldolesi J (1992) Receptor-activated  $Ca^{2+}$  influx. *J Biol Chem* 267: 2164–2172

4. Cullen PJ, Comerford JG, Dawson AP (1988) Heparin inhibits the inositol 1,4,5-trisphosphate-induced  $\text{Ca}^{2+}$  release from rat liver microsomes. *FEBS Lett* 228:57–59
5. DeLisle S, Pittet D, Potter BVL, Lew PD, Welsh MJ (1992)  $\text{InsP}_3$  and  $\text{Ins}(1,3,4,5)\text{P}_4$  act in synergy to stimulate influx of extracellular  $\text{Ca}^{2+}$  in *Xenopus* oocytes. *Am J Physiol* 262:C1456–C1463
6. Demaurex N, Lew DP, Krause KH (1992) Cyclopiazonic acid depletes intracellular  $\text{Ca}^{2+}$  stores and activates an influx pathway for divalent cations in HL-60 cells. *J Biol Chem* 267:2318–2324
7. Hallam TJ, Jacob R, Merritt JE (1988) Evidence that agonists stimulate bivalent-cation influx into human endothelial cells. *Biochem J* 255:179–184
8. Hallam TJ, Rink TJ (1985) Agonists stimulate divalent cation channels in the plasma membrane of platelets. *FEBS Lett* 186:175–179
9. Hoth M, Penner R (1992) Depletion of intracellular calcium stores activates a calcium current in mast cells. *Nature* 355:353–356
10. Hoth M, Penner R (1993) Calcium release-activated calcium current ( $I_{\text{CRAC}}$ ) in rat mast cells. *J Physiol (Lond)* (in press)
11. Irvine RF (1992) Inositol phosphates and  $\text{Ca}^{2+}$  entry: toward a proliferation or simplification? *FASEB J* 6:3085–3091
12. Jacob R (1990) Agonist-stimulated divalent cation entry into single cultured human umbilical vein endothelial cells. *J Physiol (Lond)* 421:55–77
13. Kass GEN, Llopis J, Chow SC, Duddy SK, Orrenius S (1990) Receptor-operated calcium influx in rat hepatocytes. *J Biol Chem* 265:17 486–17 492
14. Kuno M, Kimura M (1992) Noise of secretagogue-induced inward currents dependent on extracellular calcium in rat mast cells. *J Membr Biol* 128:53–61
15. Kuno M, Kawaguchi J, Mukai M, Nakamura F (1990) PT pretreatment inhibits 48/80-induced activation of  $\text{Ca}^{2+}$ -permeable channels in rat peritoneal mast cells. *Am J Physiol* 259:C715–C722
16. Kwan C-Y, Putney JW (1990) Uptake and intracellular sequestration of divalent cations in resting and methacholine-stimulated mouse lacrimal acinar cells. *J Biol Chem* 265:678–684
17. Lückhoff A, Clapham D (1992) Inositol 1,3,4,5-tetrakisphosphate activates an endothelial  $\text{Ca}^{2+}$ -permeable channel. *Nature* 355:356–358
18. Loessberg PA, Zhao H, Muallem S (1991) Synchronized oscillation of  $\text{Ca}^{2+}$  entry and  $\text{Ca}^{2+}$  release in agonist-stimulated AR42J cells. *J Biol Chem* 266:1363–1366
19. Mason MJ, Garcia-Rodriguez C, Grinstein S (1991) Coupling between intracellular  $\text{Ca}^{2+}$  stores and the  $\text{Ca}^{2+}$  permeability of the plasma membrane. *J Biol Chem* 266:20 856–20 862
20. Matthews G, Neher E, Penner R (1989) Second messenger-activated calcium influx in rat peritoneal mast cells. *J Physiol (Lond)* 418:105–130
21. Meldolesi J, Clementi E, Fasolato C, Zacchetti D, Pozzan T (1991)  $\text{Ca}^{2+}$  influx following receptor activation. *Trends Pharmacol Sci* 12:289–292
22. Missiaen L, Declerck I, Droogmans G, Plessers L, De Smedt H, Raeymaekers L, Casteels R (1990) Agonist-dependent  $\text{Ca}^{2+}$  and  $\text{Mn}^{2+}$  entry dependent on state of filling of  $\text{Ca}^{2+}$  stores in aortic smooth muscle cells of the rat. *J Physiol (Lond)* 427:171–186
23. Neher E (1989) Combined fura-2 and patch clamp measurements in rat peritoneal mast cells. In: Sellin LC, Libelius R, Thesleff S (eds) *Neuromuscular junction*. Elsevier, Amsterdam, pp 65–76
24. Ozaki Y, Yatomi Y, Kume S (1992) Evaluation of platelet calcium ion mobilization by the use of various divalent ions. *Cell Calcium* 13:19–27
25. Penner R, Matthews G, Neher E (1988) Regulation of calcium influx by second messengers in rat mast cells. *Nature* 334:499–504
26. Petersen OH (1989) Does inositol tetrakisphosphate play a role in the receptor-mediated control of calcium mobilization? *Cell Calcium* 10:375–383
27. Petersen OH (1992) Inositol tetrakisphosphate: new evidence for messenger role. *New Physiol Sci* 7:193
28. Putney JW (1990) Capacitative calcium entry revisited. *Cell Calcium* 11:611–624
29. Sage SO, Merritt JE, Hallam TJ, Rink TJ (1989) Receptor-mediated calcium entry in fura-2-loaded human platelets stimulated with ADP and thrombin. Dual-wavelength studies with  $\text{Mn}^{2+}$ . *Biochem J* 258:923–926
30. Smith PM (1992)  $\text{Ins}(1,3,4,5)\text{P}_4$  promotes sustained activation of the  $\text{Ca}^{2+}$ -dependent  $\text{Cl}^-$  current in isolated mouse lacrimal cells. *Biochem J* 283:27–30
31. Takemura H, Hughes AR, Thastrup O, Putney JW (1989) Activation of calcium entry by the tumor promoter thapsigargin in parotid acinar cells. *J Biol Chem* 264:12 266–12 271
32. Thastrup O, Cullen PJ, Drobak BK, Hanley MR, Dawson AP (1990) Thapsigargin, a tumor promoter, discharges intracellular  $\text{Ca}^{2+}$  stores by specific inhibition of the endoplasmic  $\text{Ca}^{2+}$  ATP-ase. *Proc Natl Acad Sci USA* 87:2466–2470
33. Tsien RW, Tsien RY (1990) Calcium channels, stores, and oscillations. *Annu Rev Cell Biol* 6:715–760